Supramolecular Structures of Polyethylenimine-Sodium Alkyl Sulfate Complexes

Shuiqin Zhou,[†] Christian Burger,[‡] and Benjamin Chu*[,‡]

Department of Chemistry, State University of New York at Stony Brook, Stony Brook, New York 11794, and Department of Chemistry, College of Staten Island, and The Graduate Center, The City University of New York, Staten Island, New York 10314

Received: January 15, 2004

Small-angle X-ray scattering (SAXS) has been used to investigate the supramolecular structures of complexes formed by polyethylenimine (PEI) interacting with oppositely charged surfactants of sodium alkyl sulfate (SC_nS). The effects of the alkyl chain length of the surfactants, the pH values of complex formation between PEI and SC_nS solutions, the molecular weight of branch PEI chains, and the molecular architecture of the polyelectrolyte chains have been examined. By varying these parameters for complex formation, very rich highly ordered nanostructures could be produced. The decrease in the alkyl chain length of surfactants induced a structural transition from densely packed Lamellar I to 2D distorted hexagonal packing of ribbons, then to loosely packed Lamellar II in which the alkyl chains of the surfactant were fully extended and perpendicular to the lamellar surface, and finally to a 2D hexagonal packing of cylinders. The increase in pH values of the complex formation induced a similar structural transition from a 2D rectangular face-centered (or 2D distorted hexagonal) packing of deformed cylinders to Lamellar II, and then to 2D hexagonal packing of cylinders. Both the decrease in the charge density of the PEI chains (caused by an increase in pH) and the surfactant tail length increased the ratio of the area of polar groups to the volume of alkyl chains of C_nS ions in the complexes. The structures of complexes formed by branch PEI having different molecular weights and SC_nS were compared. The packing of surfactants bound by high molecular weight branch PEI chains was less ordered in comparison with that bound by low molecular weight branch PEI chains, possibly due to the space hindrance and the rigidity of the large branch PEI chains. Three different nanostructures of Lamellar II, 2D hexagonal packing of cylinders, and $Ia\bar{3}d$ cubic were, respectively, observed when branch PEI, linear PEI and linear polyvinylamine (PVA) with similar molecular weights were used to complex with surfactants of SC_9S and $SC_{10}S$. Different chain architectures generated different charge densities and space hindrances, thereby constraining the bound surfactants in different arrangements.

Introduction

Control over the organization of nanostructures has very important technological applications, such as in electronic devices, microsensors, separation membranes, catalysts, and biomaterials.[1−4] There are widespread methods for producing highly ordered polymeric materials.[5] One of them, the complex formation between charged polyelectrolytes and oppositely charged surfactants, offers several advantages, such as straightforward preparation and isolation as well as control over supramolecular organization.[6,7] By tuning the charge density, hydrophobicity, molecular architecture, and chain flexibility of the polyelectrolyte on one hand and the properties of the surfactant on the other hand, their assembly behavior and, thus, the supramolecular structures of the resulting polyelectrolyte-surfactant complexes can be controlled within a wide range.

Most of the literature has investigated the supramolecular structures of solid (i.e., solvent-free) polyelectrolyte-surfactant complexes to explore a novel class of materials.[1,8−14] Antonietti et al.[10,11] have constructed lamellar and cylindrical superstructures, both with and without thickness undulations that were usually arranged in a highly regular periodic fashion, as well as less ordered, bicontinuous sponge phases in various solid polyelectrolyte-surfactant complexes. Thünemann et al.[10,11] determined perforated layer structures in complexes formed by silicon-containing or perfluorinated surfactants with ultralow energy surfaces. Tirrell et al.[12] observed lamellar structures in polypeptide-surfactant complexes. Ikkala et al.[13] studied a system consisting of poly(4-vinylpyridine) (PVP) and alkylphenols where, again, typical lamellar structures were produced. In contrast, the structures of water-containing polyelectrolyte-surfactant complexes were relatively less studied.

Water-equilibrated complexes might provide us with a deeper insight into the mechanisms of gene transfection and biomembrane functions because many biopolymers, such as DNAs and proteins, are polyelectrolytes, and lipids are surfactants. In recent years, the structures of water-containing polyelectrolyte-surfactant complexes have attracted increasing attention. Khokhlov et al.[15] have studied the ionic strength effect on the lamellar structure in gel-surfactant complexes between poly(diallyldimethylammonium chloride) (PDADMACl) and sodium dodecylbenzenesulfonate. In our laboratory, we have observed a structural transition from the two-dimensional (2D) hexagonal to the $Pm\bar{3}n$ cubic phase in complexes between cationic gels of PDADMACl and anionic sodium alkyl-sulfate (SC_nS) surfactants by decreasing the surfactant tail length.[16,17] Complexes between anionic hydrogels of poly(N-isopropylacrylamide−*co*-sodium methacrylate) [P(NIPAM-*co*-MAA)] and alkyl trimethylammonium bromide (C_nTAB) generated very rich nanostructures ranging from $Pm\bar{3}n$ cubic and face-centered cubic

[‡] State University of New York at Stony Brook.
[†] The City University of New York.

10.1021/jp0400317 CCC: $27.50
Published on Web 06/17/2004

over 3D hexagonal close packing of spheres to $Ia\bar{3}d$ cubic as a function of the charge density, hydrophobicity, and backbone flexibility of the polyelectrolytes and of the surfactant properties.[18−20] Furthermore, we have studied a new system of polyelectrolyte-surfactant complexes between polyvinylamine (PVA) and anionic SC_nS. Novel structures of 2D distorted hexagonal packing of deformed cylinders with various lattice parameters and pH-induced structural transitions were observed for the first time.[21]

In the present work, we have systematically investigated the supramolecular structures of water-equilibrated complexes formed by polyethylenimine (PEI) and sodium alkyl sulfates (SC_nS) by varying the alkyl chain length of SC_nS, pH values during the complex formation, as well as the molecular weight and architecture of branch PEI chains. PEI has the highest charge density of all polyelectrolytes and a strong tendency to form complexes with anionic surfactants.[22−25] Branch PEI chains are very promising as a nonviral gene delivery vehicle.[26−30] It has been reported that the transfection efficiency of DNA could be closely related to the molecular weight of branch PEI chains.[31−33] Thus, the study of nanostructures and structural transitions of water-containing PEI−SC_nS complexes under variations in pH, surfactant tail length, and molecular weight of the PEI chains could be helpful to improve our understanding of some aspects of the mechanisms of gene therapy.

In comparison with the single lamellar structure observed in solid water-free complexes formed by branch PEI chains and various surfactants,[11,14] we were able to produce very rich and highly ordered structures in water-equilibrated PEI−SC_nS complexes, including very densely packed lamellar, 2D distorted hexagonal packing of ribbons, 2D rectangular face-centered packing of deformed cylinders, loosely packed lamellae, and 2D hexagonally packed cylinders. Replacing PEI with poly(vinylamine) (PVA), that is, going from chargeable nitrogen atoms being part of the backbone to those being grafted to it, opened a phase window for $Ia\bar{3}d$ cubic double gyroid networks.

Experimental Section

Materials. Branch polyethylenimine (PEI) (M_w = 1,800, 10,000, and 70,000 g/mol), linear PEI (M_w = 25,000 g/mol), and linear poly(vinylamine) (PVA) (M_w = 25,000 g/mol) were purchased from Polyscience, Inc. The surfactants of sodium alkyl sulfate (SC_nS, n = 9−16) with n being the number of carbon atoms in the alkyl chains (Lancaster, 99%) were used without further purification. Deionized water was distilled before use. Hydrochloric acid (36.9%) and sodium hydroxide (6.25 N) from Fisher Scientific were diluted and used to adjust the pH values of the PEI, PVA, and SC_nS solutions.

Preparation of PEI−SC_nS Complexes. The complexes were prepared by dropwise addition of the PEI aqueous solution to the SC_nS aqueous solution at the desired pH values and room temperature under stirring. The PEI (or PVA) and SC_nS solutions were prepared in very dilute HCl or NaOH aqueous solution to achieve the desired pH values. The concentration of PEI was fixed at 0.018 g/mL, while the concentrations of SC_nS solutions were always kept at 1/3 of the critical micelle concentration (CMC). The volumes of the surfactant solutions were controlled at such a level that the ratio r, defined by ⟨number of surfactant molecules in solution⟩/⟨number of charged sites in the polymer chains in solution⟩, was in the range of r = 1.5. This means that the number of surfactant molecules was always in excess of the number of charged groups in the polymer chain for complex formation. The complex between PEI and SC_nS in solution became slightly cloudy. After being equilibrated with the external surfactant solution for 3 to 4 weeks, the complexes were collected by centrifuging at 6 × 10^3 g for 5 h. The complexes were always kept in equilibrium with the external surfactant solutions, even during the SAXS measurements.

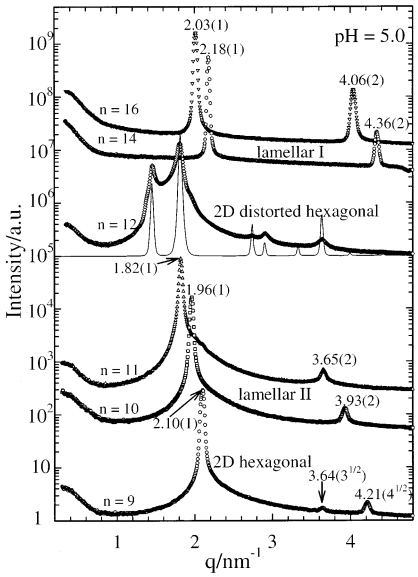

Figure 1. Typical SAXS profiles of complexes formed by low molecular weight branch PEI (M_w = 1,800 g/mol) interacting with SC_nS at different alkyl chain lengths of n = 9−16 and pH = 5.0. The solid line represents the simulation curve from the structural model of 2D distorted hexagonal packing of ribbons in Figure 2b with $a = b$ = 4.72 nm and θ = 132.9°.

X-ray Scattering Measurements. Small-angle X-ray scattering (SAXS) measurements were carried out at the Advanced Polymers Beam Line X27C at the National Synchrotron Light Source, Brookhaven National Laboratory, using a laser-aided prealigned pinhole collimator.[34] The incident beam wavelength (λ) was tuned at 0.1307 nm. Used in conjunction with a Fuji BAS2500 imaging plate scanner, as the detection system, were 2D imaging plates (Fuji). The sample to detector distance was 958 mm, corresponding to a q range of $0.6 \le q \le 5.0$ nm^{-1} with $q = (4\pi/\lambda)\sin(\theta/2)$ and θ being the scattering angle between the incident and the scattered X-ray beams. The experimental data were corrected for background scattering and sample transmission.

Results and Discussion

The centrifuged PEI−SC_nS complex precipitate had a viscous, semi-transparent and solid-like appearance. The concentrations of SC_nS were fixed at 1/3 CMC and the molar ratio of SC_nS to the polymer charge units was fixed at 1.5 for the complex formation. Therefore, it was possible that some excess surfactant molecules could be adsorbed onto the surface of the solid-like PEI−SC_nS complexes. For long tailed surfactants, their CMC is very low so that the concentration of external surfactant solution was also very low ($\sim 10^{-4}$ M).

I. Effect of Surfactant Alkyl Chain Length. Figure 1shows the SAXS profiles of complexes formed by low molecular weight branch PEI (M_w = 1,800 g/mol) interacting with SC_nS at pH = 5.0 as a function of the surfactant chain length (number of carbon atoms, n, equals 9−16). In the sequence where the alkyl chain length of the surfactants was shortened, the structures of the PEI−SC_nS complexes changed. The SAXS curves from the PEI−$SC_{16}S$ and −$SC_{14}S$ complexes showed two sharp scattering peaks with a spacing ratio of 1:2, indicating a lamellar

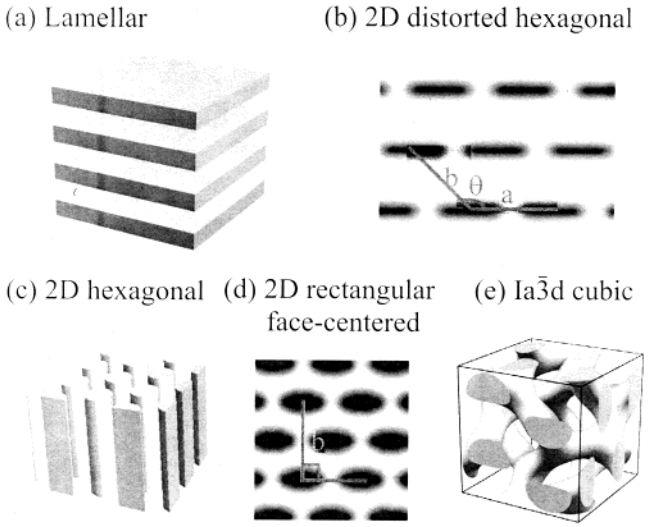

Figure 2. Structural models for lamellar, 2D distorted hexagonal packing of ribbons, 2D hexagonal packing of cylinders, 2D rectangular face-centered packing of deformed cylinders, and *Ia*$\bar{3}$*d* cubic structures observed in PEI (or PVA)−SC_nS complexes.

structure, as shown in Figure 2a. The interlayer spacing (*d*) was calculated to be 3.10 nm at $n = 16$ and 2.88 nm at $n = 14$, respectively. The increment in lamellar spacing (3.10 nm − 2.88 nm = 0.22 nm) produced by the two CH_2 groups in the surfactant alkyl chains has to include a factor of 2 in the presence of bilayers, precluding a stretched all-trans conformation in those bilayers and suggesting a large amount of interdigitation, tilting, and/or coiling with a corresponding gauche fraction.

By decreasing *n* to 12, the SAXS curve from the PEI−SC_{12}S complex showed a different structure. Five scattering peaks were observed, but without a simple regular spacing ratio as commonly observed in lamellar, hexagonal, or cubic structures. On the basis of the recently observed 2D distorted hexagonal structure packed by deformed cylinders in polyelectrolyte-surfactant complexes,[21] this SAXS curve could be attributed to a similar 2D distorted hexagonal structure. However, to approximate the relative scattering intensities in the curve, the cylinders had to be highly deformed to ribbons. Figure 2b shows a possible structural model for the cross-section of this 2D distorted hexagonal structure of the PEI−SC_{12}S complex, packed by ribbons in a primitive 2D unit cell with two equal edges ($a = b$) enclosing an angle, θ, larger than 120°. These highly deformed cylinders or ribbons were almost connected to each other, forming a layerlike structure. The solid line in Figure 1 represents the calculated scattering curve based on this structural model. All five scattering peaks from the PEI−SC_{12}S complex formed at pH = 5.0 could be reproduced by this 2D distorted hexagonal structure with two free parameters, $a = b = 4.7$ nm and $\theta = 132.9°$, giving this simple structural proposal a high level of confidence.

When the *n* value was decreased to 10 and 11, the SAXS curves showed two scattering peaks with a spacing ratio of 1:2, again indicating that the PEI−SC_{11}S and −SC_{10}S complexes also formed a lamellar structure. The interlayer spacing *d* was calculated to be 3.21 and 3.45 nm for $n = 10$ and 11, respectively. The corresponding spacing increment of 0.24 nm per CH_2 group in the bilayer period, that is, of 0.12 nm per CH_2 group in a single surfactant chain, is compatible with a mostly stretched all-trans conformation of the surfactant chains with only a slight tilt or gauche contribution to account for the difference from the ideal value. We have termed this morphology Lamellar II, in contrast to the structure Lamellar I observed

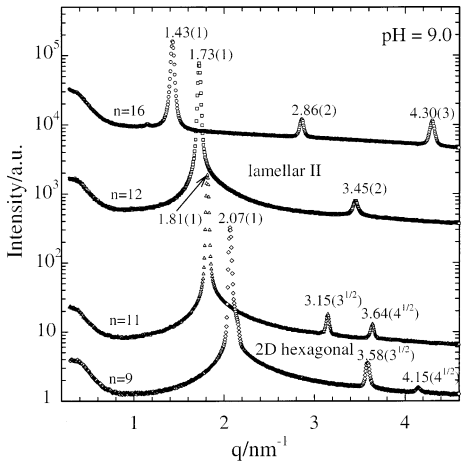

Figure 3. Typical SAXS profiles of complexes formed by low molecular weight branch PEI ($M_w = 1{,}800$ g/mol) and SC_nS at different alkyl chain lengths of $n = 9-16$ and pH = 9.0.

for the PEI−SC_{16}S and −SC_{14}S complexes discussed above. It is interesting to note that the longer alkyl chains generate the structure Lamellar I with a shorter period, whereas the higher ordering inside the bilayers formed by the shorter chains of SC_{11}S and −SC_{10}S leads to a larger period in Lamellar II. By further decreasing *n* to 9, the SAXS curve from the PVACl−SC_9S complex changed again. Three scattering peaks with a spacing ratio of $1^{1/2}:3^{1/2}:4^{1/2}$ were observed, indicating that a structure of 2D hexagonally close-packed cylinders has been formed, as shown in Figure 2c.

Thus, the length of the alkyl chains of the surfactant can determine the structure formation. The decrease in the surfactant tail length (carbon atom number *n*) has induced several structural transitions in the PEI−SC_nS complexes, from a highly interdigitated and/or tilted Lamellar I to a 2D distorted hexagonal packing of ribbons, then to a noninterdigitated Lamellar II, and finally to a 2D hexagonal packing of cylinders. It is known that the shortening of alkyl chains of surfactants increases the ratio of the area of the headgroup to the volume of the tail of the surfactant. In structures of type Lamellar I and 2D distorted hexagonal packing of ribbons formed by the long-tailed surfactants ($n = 12-16$), the alkyl chains of the surfactant could be tilted relative to the normal interface. In the structure of type Lamellar II formed at $n = 10-11$, the alkyl chains could be more fully extended and perpendicular to the lamellar surface. The morphology of 2D hexagonal close packing cylinders formed at $n = 9$ suggests an inversion of the structure in the sense that the cylinders in the 2D hexagonal structure were filled by the hydrophobic nonyl chains, while the hydrophilic phase of PEI chains, the sulfate groups, and water form the enclosing matrix.

Figure 3 shows the SAXS profiles of complexes formed by the same low molecular weight branch PEI ($M_w = 1{,}800$ g/mol) interacting with SC_nS ($n = 9-16$) but at a different pH value of 9.0. Again, the decrease in the carbon atom number of the alkyl chains induced a structural transition of the PEI−SC_nS complexes. The SAXS curve from the PEI−SC_{16}S complex showed three peaks with a spacing ratio of 1:2:3, indicating a lamellar structure. By decreasing *n* to 12, a similar lamellar structure was observed. The interlayer spacing *d* was calculated to be 4.42 nm at $n = 16$ and 3.63 nm at $n = 12$, respectively. The difference in lamellar spacing produced by one CH_2 group in the surfactant tails was equal to 0.20 nm. In terms of the bilayer arrangement of C_nS, this difference corresponds to a spacing increment of 0.10 nm per CH_2 group, suggesting that

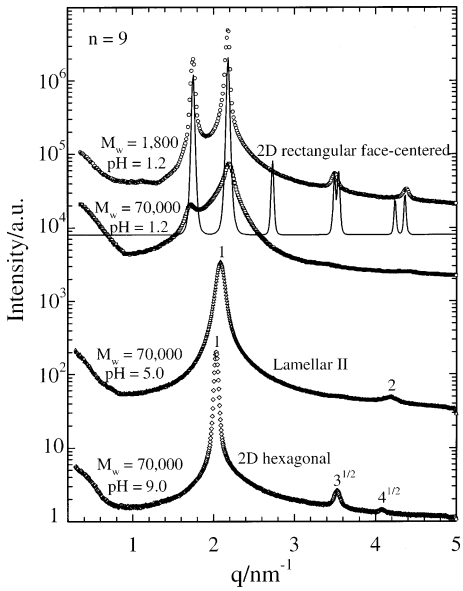

Figure 4. Typical SAXS profiles of branch PEI−SC_9S complexes formed at three different pH values of 1.2, 5.0, and 9.0, respectively. The solid line represents the simulation curve from the structural model of 2D rectangular face-centered packing of deformed cylinders in Figure 2d with $a = 4.60$, $b = 5.76$ nm, and $\theta = 90°$.

the alkyl chains of surfactants in the lamellar structure were mostly extended and we would assign this structure to the Lamellar II type. When n was decreased from 12 to 11, the SAXS curve of the PEI−$SC_{11}S$ complex changed. Three sharp scattering peaks with a spacing ratio of $1^{1/2}$:$3^{1/2}$:$4^{1/2}$ were observed, indicating a structure of 2D hexagonal close packed cylinders. By further decreasing n to 9, the 2D hexagonal structure was retained but with a smaller d-spacing. Thus, the decrease in n values of SC_nS from 16 to 9 induced only one structural transition of the PEI−SC_nS complexes formed at pH = 9.0 from Lamellar II to a 2D hexagonal packing of cylinders. This showed that this phase behavior was much simpler in comparison with the plentiful structural transitions of these PEI−SC_nS complexes formed at pH = 5.0, as shown in Figure 1, for the same lengths of the alkyl chains being shortened from n = 16 to n = 9. This shows that the pH values for the complex formation between PEI and SC_nS also determine the structure formation of the PEI−SC_nS complexes.

II. Effect of pH Values for Complex Formation between PEI and SC_nS Solutions. Figure 4 shows the SAXS profiles of complexes formed between high molecular weight branch PEI (M_w = 70,000 g/mol) and SC_9S at pH = 1.2, 5.0, and 9.0, respectively. When the complex was formed at pH = 1.2, only two scattering peaks were observed. It was difficult to identify the structure by this SAXS curve alone. To identify the structure, the SAXS curve from the complex formed by low molecular weight branch PEI (M_w = 1,800 g/mol) and SC_9S at pH = 1.2 is also shown in Figure 4 for comparison. Four sharp scattering peaks were observed, but did not show a simple spacing ratio. However, all the peaks could be fitted by a structure of 2D rectangular face-centered packing of deformed cylinders. Figure 2d shows a possible structural model for this special structure with two deformed cylinders per unit cell. The solid curve in Figure 4 represents the calculated curve based on this structural model with lattice parameters of $a = 4.60$ nm, $b = 5.76$ nm, and an enclosing right angle of $\theta = 90.0°$. Although the two scattering peaks in the SAXS curve of the complex formed by the high molecular weight branch PEI (M_w = 70,000 g/mol) were broader and relatively weaker, the peak positions and the relative intensities of the first two peaks were consistent. We speculate that the complex formed between the high molecular weight branch PEI (M_w = 70,000 g/mol) and SC_9S at pH = 1.2 had the same type structure of 2D rectangular face-centered packing of deformed cylinders as that formed by the low molecular weight branch PEI (M_w = 1,800 g/mol), but the packing could be less orderly because of the space hindrance from the high molecular weight branch chains. When the complex between the high molecular weight branch PEI (M_w = 70,000 g/mol) and SC_9S was formed at pH = 5.0, the SAXS curve became much simpler. Two scattering peaks at $q = 2.09$ and 4.19 nm^{-1} in the curve could be indexed as the first two orders of a layered structure. This lamellar structure should belong to Lamellar II as discussed in Figure 1. By further increasing the pH value in the complex formation between PEI and SC_9S solutions to 9.0, three scattering peaks with a spacing ratio of $1^{1/2}$:$3^{1/2}$:$4^{1/2}$ were observed, indicating that a structure of 2D hexagonal close packing of cylinders was formed. It can be seen that if all the other conditions were fixed, the gradual increase in pH values from 1.2 to 9.0 for the complex formation between PEI and SC_9S solutions could induce a structural transition of the complexes from a 2D rectangular face-centered packing of deformed cylinders to a multibilayer lamellar structure, and finally to a 2D hexagonal close packing of cylinders.

An increase in the pH value of the PEI solution would decrease the charge density on PEI chains, but increase the neutral sites on the chains. These neutral sites were hydrophilic and should be favored on the aqueous phase. Therefore, when the pH value in the complex formation was increased, the headgroups of the surfactant ions arranged inside the complexes could be more swollen by water. This means that when the complexes were formed at higher pH values, the C_nS surfactants bound by the oppositely charged PEI chains would have a larger ratio of the area of the headgroup to the volume of the alkyl chains, thus having larger mean interfacial curvature between the hydrophilic moieties and the hydrophobic tails of the surfactant in the complexes. This pH-induced increase in interfacial curvature of surfactants arranged inside the complexes was similar to the effect of the shortening of alkyl chain length of the surfactants, thus inducing a similar structural transition from the 2D rectangular face-centered packing of deformed cylinders (or 2D distorted hexagonal packing of deformed cylinders upon different unit cell selection) to Lamellar II, and then to 2D hexagonal packing of cylinders.

III. Effect of Molecular Weight of Branch PEI Chains. Figure 5 shows the SAXS profiles of complexes formed by different molecular weight branch PEI chains interacting with $SC_{12}S$ or $SC_{11}S$ at pH = 5.0, respectively. These SAXS curves indicated that the increase in molecular weight of branch PEI chains alone could significantly affect the structural formation of PEI−SC_nS complexes. Under the same complex formation conditions of pH = 5.0 and n = 12, the PEI−$SC_{12}S$ complex formed by low molecular weight branch PEI chains (M_w = 1,800 g/mol) produced a 2D distorted hexagonal structure, as shown in Figure 2b, packed by highly deformed cylinders or ribbons. When the molecular weight of the branch PEI chains was increased to 10,000 g/mol, the sharp scattering peaks in the SAXS curve of the PEI−$SC_{12}S$ complex disappeared. Only the first two most intense peaks were still visible and presented as broad shoulder peaks. The structure of this PEI−$SC_{12}S$ complex formed by the medium molecular weight branch PEI chains (M_w = 10,000 g/mol) might still belong to a 2D distorted hexagonal packing of highly deformed ribbons, but the packing of the

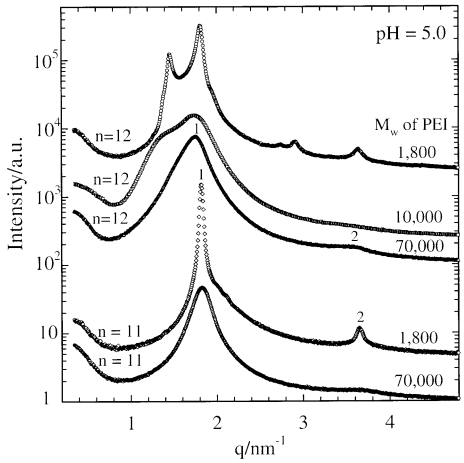

Figure 5. Typical SAXS profiles of complexes formed by different molecular weight branch PEI chains interacting at pH = 5.0 with $SC_{12}S$ and $SC_{11}S$, respectively.

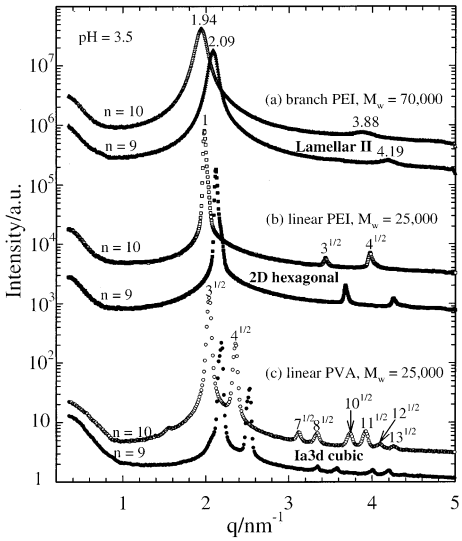

Figure 6. Typical SAXS profiles of complexes formed by branch PEI, linear PEI, and linear PVA chains with different molecular architectures interacting with the same surfactants of $SC_{10}S$ and SC_9S at pH = 3.5, respectively.

ribbons from the self-assembly of the surfactant became much less ordered. By further increasing the molecular weight of branch PEI chains to 70,000 g/mol, the SAXS curve of the PEI−$SC_{12}S$ complex completely changed. Two broad scattering peaks at $q = 1.74$ and 3.49 nm^{-1} appeared. These two peaks had a spacing ratio of 1:2, indicating that a lamellar structure in the complex had been formed. Obviously, an increase in the molecular weight of branch PEI chains induced a structural transition of PEI−$SC_{12}S$ complexes. When $SC_{11}S$ was used to complex with different molecular weight branch PEI chains, only a lamellar structure was formed. However, the increase in the molecular weight of branch PEI chains still affected the packing order of the lamellar structure. The SAXS curve from the complex formed by low molecular weight branch PEI chains (M_w = 1,800 g/mol) showed strong and sharp scattering peaks, while the scattering peaks from the complex formed by high molecular weight branch PEI chains (M_w = 70,000 g/mol) were much broader and weaker. This means that the lamellar structure of the low molecular weight PEI−$SC_{11}S$ complex showed a higher degree of long-range order and/or a larger stack size compared to the high molecular weight PEI−$SC_{11}S$ complex.

Our experimental results have proven that the molecular weight of branch PEI chains had a tremendous effect on the structures of PEI−SC_nS complexes. The increase in the molecular weight of branch PEI chains could increase the rigidity of PEI chains and space hindrance so that the arrangement of the C_nS surfactants bound by these PEI chains changed. The molecular weight dependence of the structures of PEI−SC_nS complexes could be helpful to understand the mechanism of DNA delivery by using branch PEI chains as a delivery vehicle. It has been shown that the DNA transfection efficiency highly depended on the molecular weight of branch PEI chains as a carrier.[31−33] Although the supramolecular structures of PEI−SC_nS complexes could be quite different from those of PEI-DNA complexes due to the different conformations of small SC_nS molecules and rigid DNA chains, we believe that the molecular weight-induced transfection efficiency variance of branch PEI as a gene delivery vehicle is related to the structures of PEI-DNA complexes.

IV. Effect of Polymer Chain Architectures. Figure 6 shows three groups of SAXS curves from the complexes formed by branch PEI, linear PEI, and linear PVA chains of similar molecular weights interacting with SC_9S and $SC_{10}S$ at pH = 3.5, respectively. The SAXS curves of branch PEI−$SC_{10}S$ and −SC_9S complexes showed two scattering peaks with a spacing ratio of 1:2, indicating a lamellar structure. The lamellar spacing decreased when n was decreased from 10 to 9. In terms of a bilayer arrangement, the average spacing increment per CH_2 group in the alkyl chains of $C_{10}S$ and C_9S packed inside the complexes could be calculated to be 0.12 nm, suggesting that the alkyl chains of the surfactants were fully stretched. Therefore, the lamellar structure in the branch PEI−$SC_{10}S$ and −SC_9S complexes could be identified as Lamellar II. When the branch PEI chains (M_w = 70,000 g/mol) were changed to linear PEI chains (M_w = 25,000 g/mol), the SAXS curves from the linear PEI−$SC_{10}S$ and −SC_9S complexes changed. Three sharp scattering peaks with a spacing ratio of $1^{1/2}$:$3^{1/2}$:$4^{1/2}$ could be identified as a typical structure of 2D hexagonal close packing of cylinders. The structural transition from Lamellar II to 2D hexagonal packing of cylinders could be attributed to the different PEI chain architecture, for example, branch versus linear. Branch PEI chains had a lower charge density (i.e., only about 2/3 of the nitrogen atoms could be protonated) and a more rigid conformation in comparison with linear PEI chains. The surfactants bound by the rigid branch PEI chains could self-assemble to a bilayer lamellar structure with zero mean curvature, while the surfactant ions bound by the flexible linear PEI chains could still form cylinders with a positive mean curvature because the flexible PEI chains could wrap onto the surface of cylinders.

To further investigate the polymer chain architecture effect on the structures of polyelectrolyte-surfactant complexes, linear PVA chains (M_w = 25,000 g/mol) were also used to complex with $SC_{10}S$ and SC_9S under the same conditions. The repeating units of linear PEI and linear PVA chains have the same molecular weight, but the architecture is quite different. In linear PEI chains, the −NH− is part of the backbone chain and there is one chargeable unit per three bonds on the backbone chain. In linear PVA chains, the $-NH_2$ is grafted onto the backbone chain and there is one chargeable unit per two bonds on the backbone chain. This difference in polymer chain architecture could produce very different structures in the formed complexes when they were interacting with the same oppositely charged surfactants under otherwise identical conditions. For example, the SAXS curves from the linear PVA−$SC_{10}S$ and −SC_9S complexes showed eight scattering peaks with a spacing ratio of $3^{1/2}$:$4^{1/2}$:$7^{1/2}$:$8^{1/2}$:$10^{1/2}$:$11^{1/2}$:$12^{1/2}$:$13^{1/2}$. This indicated that a

cubic phase structure of the $Ia\bar{3}d$ space group, that is, of the double gyroid type, was formed. The corresponding diffraction peaks can be indexed as 211, 220, 321, 400, 420, 332, 422, and 510/431. The $Ia\bar{3}d$ cubic structure has been very commonly observed in lipid/water binary systems in a region of the phase diagram between the lamellar and the hexagonal phase.[35] However, it was rarely observed in polyelectrolyte-surfactant complexes. Figure 2e shows the structural model of $Ia\bar{3}d$ cubic, consisting of two infinite 3D networks, mutually intertwined but unconnected, which could be idealized by a skeleton graph consisting of coplanarly joined rods.[35,36] At pH = 3.5, most of the amine groups can be protonated so that the charge density of the PVA chains is very high. Furthermore, the $-NH_3^+$ groups are very close to the backbone chains, thus the headgroups of the $C_{10}S$ and C_9S surfactants bound by the PVA chains would compact very densely and form the distorted rods in the $Ia\bar{3}d$ cubic structure. In contrast, the relatively lower charge density in the linear PEI chains permits more space for $C_{10}S$ and C_9S to pack into cylinders in the 2D hexagonal structure.

Conclusions

Very rich highly ordered supramolecular nanostructures could be produced by the complex formation between PEI chains and oppositely charged SC_nS surfactants under various conditions. Both the decrease in alkyl chain length of surfactants and the increase in pH values of the complex formation between branch PEI and SC_nS solutions could induce a similar structural transition from densely packed Lamellar I to 2D distorted hexagonal packing of highly deformed cylinders, then to Lamellar II in which the alkyl chains of the surfactant were fully extended and perpendicular to the lamellar surface, and finally to a 2D hexagonal packing of cylinders. This structural transition could be partially attributed to the increase in mean curvature at the polar/nonpolar interface (or the ratio of area of the polar group to volume of the alkyl chains). In addition, the molecular weight of branch PEI chains could also significantly affect the structures of the formed PEI$-SC_nS$ complexes. The structures of complexes formed by high molecular weight branch PEI were less ordered in comparison with those formed by low molecular weight branch PEI chains, possibly due to the space hindrance and rigidity of the high molecular weight branch PEI chains. Furthermore, the chain architecture of polyelectrolytes was also very important in constraining the self-assembly of bound surfactant ions. The complexes formed by rigid branch PEI with $SC_{10}S$ and SC_9S prefer to form the Lamellar II phase, while the complexes formed by flexible linear PEI with $SC_{10}S$ and SC_9S can form a 2D hexagonal phase with the PEI chains surrounding on the surface of cylinders. By replacing the $-NH-$ group in the backbone chain of linear PEI with the $-NH_2$ group pendent on the backbone chain of linear PVA, the 2D hexagonal phase transferred to a $Ia\bar{3}d$ cubic structure because of the different charge density and space hindrance between linear PEI and PVA chains.

Acknowledgment. B.C. gratefully acknowledges the support of this work by the Polymer Program, the National Science Foundation (DMR9984102), and the Department of Energy for beamline support of X27C (DEFG0299ER45760) at NSLS, BNL.

References and Notes

(1) Ober, C. K.; Wegner, G. *Adv. Mater.* **1997**, *9*, 17 and references therein.
(2) Zhou, S. Q.; Chu, B. *Adv. Mater.* **2000**, *12*, 545.
(3) Scott, B. J.; Wirnsberger, G.; Stucky, G. D. *Chem. Mater.* **2001**, *13*, 3140.
(4) de Soler-lllia, A. A. G. J.; Sanchez, C.; Lebean, B.; Patariu, J. *Chem. Rev.* **2002**, *102*, 4093.
(5) Liu, T.; Burger, C.; Chu, B. *Prog. Polym. Sci.* **2003**, *28*, 5.
(6) Hayakawa, K.; Kwak, J. C. T. *Cationic Surfactants*; Rubingh, D. N., Holland, P. M., Eds.; Marcel Dekker: New York, 1991; pp 189−248.
(7) Goddard, E. D.; Ananthapadmanabhan, K. P. *Interactions of Surfactants with Polymers and Proteins*; CRC Press: Boca Raton, FL, 1993.
(8) Antonietti, M.; Maskos, M. *Macromolecules* **1996**, *29*, 4199.
(9) Antonietti, M.; Radloff, D.; Wiesner, U.; Spiess, H. W. *Macromol. Chem. Phys.* **1996**, *197*, 2713.
(10) Thunemann, A. F.; Lochhaas, K. H. *Langmuir* **1998**, *14*, 6220; **1999**, *15*, 4867.
(11) Thunemann, A. F. *Langmuir* **2000**, *16*, 824.
(12) Ponomarenko, E. A.; Tirrell, D. A.; MacKnight, W. J. *Macromolecules* **1998**, *31*, 1584.
(13) Ruokolainen, J.; Tanner, J.; Ikkala, O.; ten Brinke, G.; Thomas, E. L. *Macromolecules* **1998**, *31*, 3532.
(14) Chen, H. L.; Hsiao, M. S. *Macromolecules* **1999**, *32*, 2967.
(15) Mironov, A. V.; Starodoubtsev, S. G.; Khokhlov, A. R.; Dembo, A. T.; Yakunin, A. N. *Macromolecules* **1998**, *31*, 7698.
(16) Sokolov, E. L.; Yeh, F.; Khokhlov, A. R.; Chu, B. *Langmuir* **1996**, *12*, 6229.
(17) Yeh, F.; Solokov, E. L.; Khokhlov, A. R.; Chu, B. *J. Am. Chem. Soc.* **1996**, *118*, 6615.
(18) Zhou, S. Q.; Burger, C.; Yeh, F.; Chu, B. *Macromolecules* **1998**, *31*, 8157.
(19) Zhou, S. Q.; Yeh, F. J.; Burger, C.; Chu, B. *J. Polym. Sci., Polym. Phys. Ed.* **1999**, *37*, 2165.
(20) Zhou, S. Q.; Yeh, F. J.; Burger, C.; Chu, B. *J. Phys. Chem. B* **1999**, *103*, 2107.
(21) Zhou, S. Q.;Hu, H. B.; Burger, C.; Chu, B. *Macromolecules* **2001**, *34*, 1772.
(22) Meszaros, R.; Thompson, L.; Bos, M.; Varga, I.; Gilanyi, T. *Langmuir* **2003**, *19*, 609.
(23) EI-khouri, R. J.; Johal, M. S. *Langmuir* **2003**, *19*, 4880.
(24) Winnik, M. A.; Bystryak, S. M.; Chassenieux, C.; Strashko, V.; Macdonald, P. M.; Siddiqui, J. *Langmuir* **2000**, *16*, 4495.
(25) Windsor, R.; Neivandt, D. J.; Davies, P. B. *Langmuir* **2002**, *18*, 2199.
(26) Garnett, M. C. *Critical Reviews in Therapeutic Drug Carrier Systems* **1999**, *16*, 147.
(27) Tseng, W. C.; Jong, C. M. *Biomacromolecules* **2003**, *4*, 1277.
(28) Merdan, T.; Callahan, J.; Petersen, H.; Kunath, K.; Bakowsky, U.; Kopeckova, P.; Kissel, T.; Kopecek, J. *Bioconjugate Chem.* **2003**, *14*, 989.
(29) Wang, D. A.; Narang, A. S.; Kotb, M.; Gaber, A. O.; Miller, D. D.; Kim, S. W.; Mahato, R. I. *Biomacromolecules* **2002**, *3*, 1197.
(30) Pun, S. H.; Davis, M. E. *Bioconjugate Chem.* **2002**, *13*, 630.
(31) Godbey, W. T.; Wu, K. K.; Mikos, A. G. *J. Biomed. Mater. Res.* **1999**, *45*, 268.
(32) Fischer, D.; Bieber, T.; Li, Y. X.; Elsasser, H. P.; Kissel, T. *Pharm. Res.* **1999**, *16*, 1273.
(33) Kursa, M.; Walker, G. F.; Roessler, V.; Ogris, M.; Roedl, W.; Vircheis, R.; Wagner, E. *Bioconjugate Chem.* **2003**, *14*, 222.
(34) Chu, B.; Harney, P. J.; Li, Y.; Linliu, K.; Yeh, F.; Hsiao, B. S. *Rev. Sci. Instrum.* **1994**, *65*, 597.
(35) Mariani, P.; Luzzati, V.; Delacroix, H. *J. Mol. Biol.* **1988**, *204*, 165.
(36) Seddon, J. M. *Biochim. Biophys. Acta* **1990**, *1031*, 1.